

NJC

Accepted Manuscript



This is an *Accepted Manuscript*, which has been through the Royal Society of Chemistry peer review process and has been accepted for publication.

Accepted Manuscripts are published online shortly after acceptance, before technical editing, formatting and proof reading. Using this free service, authors can make their results available to the community, in citable form, before we publish the edited article. We will replace this *Accepted Manuscript* with the edited and formatted *Advance Article* as soon as it is available.

You can find more information about *Accepted Manuscripts* in the [Information for Authors](#).

Please note that technical editing may introduce minor changes to the text and/or graphics, which may alter content. The journal's standard [Terms & Conditions](#) and the [Ethical guidelines](#) still apply. In no event shall the Royal Society of Chemistry be held responsible for any errors or omissions in this *Accepted Manuscript* or any consequences arising from the use of any information it contains.

Theoretical study on homolytic C(sp²)-O cleavage in ethers and phenols

Lanlan Ding, Wenrui Zheng*, Yingxing Wang

College of Chemistry and Chemical Engineering, Shanghai University of
Engineering Science, Shanghai 201620, China

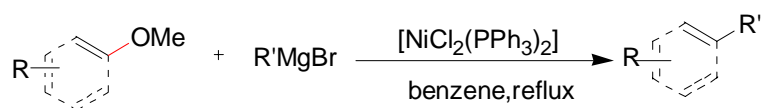
Abstract: The C-O homolytic bond dissociation enthalpies(BDEs) of many ethers were calculated by high-level *ab initio* methods including G4, G3, CBS-Q, CBS-4M as well as 26 density function theory (DFT) methods. Among the DFT methods, the wB97 provided the most accurate results and the root mean square error (RMSE) is 9.3 kJ/mol for 72 C-O BDE calculations. Therefore, an extensive C(sp²)-O BDEs and the substituent effect of alkenyl ethers, *para*-position phenyl ethers/phenols as well as several typical heterocyclic ethers were investigated in detail by wB97 methods, which is important for the understanding of the chemical process involved in the cross-coupling reactions. For alkenyl ethers, the different substituents exhibited significant effects on C(sp²)-O BDEs, especially, the conjugate effect of the substituents on O atom can greatly decrease the C(sp²)-O BDEs. In addition, the NBO analysis produced good linear correlations between the C(sp²)-O BDEs and $q_C \times q_O$ values (the q_C and q_O values denoted the natural charge of C and O atom of C-O bond respectively). For *para*-position phenyl ethers and phenols, excellent linear relationships between the C(sp²)-O BDEs with substituent constant σ_p^+ are found. The further discussion of the substituent effect separated into the ground effect and radical effect can further help us to understand the essence. For several five-membered typical heterocyclic ethers, the larger bond angle change will lead to a smaller C-O BDE.

1. Introduction

The transition-metal catalyzed cross-coupling reactions involving C(sp²)-O cleavage have been attracting much interest in organic synthesis.¹ The ethers/phenols are relatively common organic compounds containing C-O bond. Recently, there are lots of experimental researches on the C(sp²)-O activation reactions in ethers and phenols by various transition metal catalysts (in particular Ni), in which different C-C bonds can be constructed.² For instance, Wenkert et al. first introduced the Kumada-Tamao-Corriu cross-coupling of enol ethers, aryl ethers and Grignard reagents by the [NiCl₂-(PPh₃)₂] catalyst (Scheme 1),³ which has been applied to synthesize useful molecules.⁴ Lately, Johnstone and Mclean reported the Kumada-Tamao-Corriu

* Corresponding author. Tel.: +86 21 67791216; fax: +86 21 67791220.
E-mail address: wrzheng@sues.edu.cn (W.R. Zheng).

crossing-coupling of aryl tetrazolyl ethers with Grignard reagents by nickel catalyst and it is found that the phenyl substrates can give good yields.⁵ Recently, Shi et al. studied a practical nickel-catalyzed methylation of aryl methyl ethers and the desired products with high yields can be obtained.⁶ Chatani et al. developed a Suzuki-Miyaura crossing-coupling reaction of aryl methyl ethers with boronic esters without directing-group assistance.⁷ Chatani et al. also explored Buchwald-Hartwig amination of anisoles with amines by using a NHC ligand under the condition of nickel catalyst, which offered an alternative route to synthesize aryl amines.⁸ In addition, Shi et al. developed the first example of the cross-coupling of 2-naphthol derivatives with aryl Grignard reagents, and various substituted naphthols underwent the reaction well.⁹



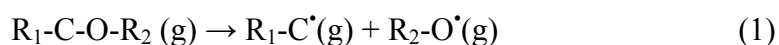
Scheme 1. Nickel-catalyzed cross-coupling reaction of methyl enol/aryl ether.

Obviously, the $\text{C}(\text{sp}^2)\text{-O}$ homolytic bond dissociation enthalpy (BDE) values, which can describe the strength of the bond in ether/phenols from the thermodynamic viewpoint, are useful for better understanding of the C-O activation and more effective substrates selection. However, on the one hand, we found that the experimental $\text{C}(\text{sp}^2)\text{-O}$ BDEs in ether/phenols are very scarce after consulting various thermodynamic database, which is perhaps due to the complexity and the laboriousness of current experimental conditions to measure the BDEs. On the other hand, although the rapid development of computational chemistry can provide us a wide variety of methods to evaluate BDEs with high precision,¹⁰ the theoretical investigations on C-O BDEs in ethers/phenols are rarely reported. Relevantly, Pratt et al. calculated the $\text{C}(\text{sp}^3)\text{-O}$ BDEs in gas phase for substituted anisoles, benzyl 4-substituted phenyl ethers and 4-substituted benzyl phenyl ethers by using density function theory (DFT) methods.¹¹

In the present study, the C-O BDEs in ethers were systematically calculated by using theoretical procedures, including high-level composite *ab initio* method and DFT methods. Afterwards, an extensive $\text{C}(\text{sp}^2)\text{-O}$ BDEs and the substituent effect of alkenyl ethers, *para*-position phenyl ethers/phenols as well as several typical heterocyclic ethers are investigated in detail.

2. Computational method

The C-O bond dissociation enthalpy (BDE) is known as the enthalpy change in the gas phase at 298.15K, 1atm in the following reaction:¹²



The enthalpy of each species can be calculated from the equation:

$$H(298K) = E + ZPE + H_{trans} + H_{rot} + H_{vib} + RT \quad (2)$$

In this equation, ZPE is the zero point energy; H_{trans} , H_{rot} , and H_{vib} are the standard temperature correction terms calculated with equilibrium statistical mechanics with harmonic oscillator and rigid rotor approximations.¹³

Four composite high-level *ab initio* methods of G4,¹⁴ G3,¹⁵ CBS-Q,¹⁶ CBS-4M¹⁷ were selected to calculate the C-O BDEs in ethers with experimental values, in which less than 8 non-hydrogen atoms are contained.

It should be noted that in all of the DFT calculations, the geometry optimization is conducted at the B3LYP/6-31+G(d) level, which is a good choice for structure optimization for its high accuracy and reasonable computing resource demands.¹⁸ Frequency calculations were performed at the same level, in which, the correct nature of the stationary points was confirmed and the zero-point vibrational energies (ZPE) were also extracted. Afterwards, a series of DFT methods were applied to single point calculations including B3P86,¹⁹ BMK,²⁰ M05,²¹ BH&HLYP,²² B3LYP,²³ M06-L,²⁴ TPSS1KCIS,²⁵ B97-1,²⁶ B97-2,²⁷ B98,²⁸ wB97,²⁹ wB97X,²⁹ wB97X-D,³⁰ PBE1PBE,³¹ MPW1P86,³² MPW1B95,³³ MPWCIS1K,³⁴ B97-D,³⁵ MPW1K,³⁶ MPWB1K,³³ MPWLYP1M,³⁷ MPW1KCIS,³⁴ CAM-B3LYP,³⁸ B3LYP-D3,³⁹ B97-D3,⁴⁰ M06-2X.⁴¹ The basis set for the single-point energies calculation is 6-311++G (2df,2p).

All above the calculations were performed using the Gaussian 09 programs.⁴²

3. Results and discussion

3.1 Assessment of the composite high-level methods

Considering the high accuracy of composite high-level methods, such as Gaussian-n (Gn) models,⁴³ complete-basic-set(CBS)⁴⁴ procedures, in the thermodynamic properties calculations including BDEs,⁴⁵ we chose four methods (G4, G3, CBS-Q and CBS-4M) for C-O BDEs assessment. The theoretical results can give us the information of the self-consistency of different composite methods as well as the re-evaluation of the experimental values. In our benchmark, 19 experimental C-O BDEs in ethers (less than 8 non-hydrogen atoms) compiled from Luo's Comprehensive Handbook of Chemical Bond Energies⁴⁶ are included, in which most of them belong to C(sp³)-O type due to the inadequacy of the experimental values of C(sp²)-O. The results of four composite *ab initio* methods as well as the experimental ones are listed in Table 1. And the correlations between theoretical BDEs with experimental ones denoted by mean deviation (MD), mean absolute deviation (MAD) and root mean square error (RMSE) that are also presented in the table.

As shown in Table 1, for the 19 C-O BDE calculations, there are good self-consistencies for these four theoretical methods. Among all of the BDEs by four methods, the largest discrepancy is 19.9 kJ/mol between G4 and CBS-4M in the C-O

bond of 1-ethoxy-propane (No. 11). In addition, the RMSE value of G4 method is the smallest of 6.5 kJ/mol, and the MD and MAD are -4.9 and 5.6 kJ/mol respectively. The results indicated that the composite G4 method can provide desirable C-O BDEs in ethers. Similarly, in the research of Curtiss, the average absolute deviation of G4 is only 0.83 kcal/mol for a set of 454 energies calculation.¹⁴ The RMSE of G3 is the second smallest of 6.9 kJ/mol, and the MD and MAD are -0.2 and 5.8 kJ/mol separately. By comparison, RMSE values of the two CBS methods are larger (over 10 kJ/mol). The similar phenomenon was found in our previous study.⁴⁷

Table 1. The C-O BDEs of ethers by four composite methods (kJ/mol)

No.	Compounds	Exp	G4	G3	CBS-Q	CBS-4M
1	H ₃ C-OCH ₃	349.8±4.2	346.8	348.3	354.9	361.4
2	H ₃ C-OC ₂ H ₅	348.1±4.2	347.1	349.2	356.1	362.7
3	C ₂ H ₅ -OCH ₃	353.1±5.4	355.8	360.8	366.5	370.5
4	C ₂ H ₃ -OC ₂ H ₃	326.8±10.5	317.8	318.3	327.1	330.7
5	C ₂ H ₅ -OC ₂ H ₃	272.8±10.5	264.8	265.2	274.0	275.2
6	C ₂ H ₅ -OC ₂ H ₅	355.6±6.3	352.9	361.6	367.6	371.7
7	nC ₃ H ₇ -OCH ₃	356.5±6.3	346.5	356.2	362.5	365.9
8	H ₃ C-OiC ₃ H ₇	350.2±6.3	346.5	350.4	356.5	363.5
9	iC ₃ H ₇ -OCH ₃	358.6±4.2	357.1	365.1	369.4	372.1
10	C ₂ H ₅ -OC ₃ H ₇	358.4±8.4	354.0	361.4	369.3	373.4
11	C ₃ H ₇ -OC ₂ H ₅	355.2±8.4	352.4	362.6	370.5	372.3
12	C ₃ H ₇ -OC ₂ H ₃	274.1±10.5	264.3	266.2	276.7	276.1
13	C ₄ H ₉ -OCH ₃	343.9±6.3	348.7	359.4	365.7	368.1
14	H ₃ C-OC ₄ H ₉	353.1±6.3	345.0	346.0	357.9	363.1
15	C ₂ H ₅ O-C ₃ H ₇	356.9±6.3	352.4	362.6	370.5	372.3
16	C ₂ H ₃ -OC ₄ H ₉	419.2±8.4	411.5	415.9	427.8	430.4
17	C ₄ H ₉ -OC ₂ H ₃	273.2±10.5	263.9	266.9	278.4	275.9
18	tC ₄ H ₉ -OC ₂ H ₅	347.3±6.3	335.9	344.2	352.3	354.4
19	C ₂ H ₅ -OtC ₄ H ₉	349.6±6.3	346.6	338.7	361.3	364.9
	MD	—	-4.9	-0.2	8.6	11.7

MAD	–	5.6	5.8	8.6	11.7
RMSE	–	6.5	6.9	10.1	13.1

Note: MD (mean deviation) = $\sum(x_i - y_i)/N$; MAD (mean absolute deviation) = $\sum|x_i - y_i|/N$; RMSE (root mean square error) = $[\sum(x_i - y_i)^2/N]^{1/2}$ ($N = 19$, x_i represents the calculated data for each species, and y_i represents the experimental data accordingly).

3.2 Assessment of different DFT methods

Although the G4 method can provide accurate C-O BDEs for ethers, it is only suitable for the calculation of the small system. The density functional theory (DFT) is popularly believed to be a good choice for BDE calculation because of the no serious spin-contamination and relatively low CPU-cost, which is applicable for large systems with desirable precision.⁴⁸

Besides the 19 C-O BDEs in Table 1, we extended our benchmark by adding 53 C-O BDEs with experimental values in larger systems. Afterwards, the 26 DFT methods, in which the exchange-correlation functional like BMK, M05, the long-range corrected hybrid density functional such as wB97, wB97X and some functionals with dispersion correction (wB97X-D, B97-D, B3LYP-D3 and B97-D3) are selected to calculate the 72 C-O BDEs of ethers. All of the results are shown in the Supporting Information, and the MD, MAD and RMSE values of the 26 DFTs are listed in the Table 2.

Among all of the DFT methods from the Table 2, for 72 C-O BDEs calculation of ethers, the wB97 method gave the highest accuracy with the smallest RMSE value (9.3 kJ/mol), and the MD and MAD are -2.4 kJ/mol and 8.2 kJ/mol respectively, which illustrated that there are both positive and negative deviations comparing with experimental values for these C-O BDE calculation. The second and the third superior methods are BMK and wB97X with the RMSE values of 11.3 and 11.7 kJ/mol separately. As the one of the most popular method, B3LYP presents the largest RMSE value of 45.4 kJ/mol and underestimated all of the 72 C-O BDE values. Hence, B3LYP cannot be directly used for C-O BDE calculation in ethers although it can give appealing performance for some organic compounds.⁴⁹ Compared with B3LYP method, the newer CAM-B3LYP and dispersion correction functional B3LYP-D3 method can greatly improve the accuracy for 72 C-O BDEs (the RMSE values are 19.4 kJ/mol and 19.9 kJ/mol separately).

In addition, we calculated the 72 C-O BDEs at the wB97/6-311++G(2df,2p)//wB97/6-31+G(d) level, and the results are also listed in this table(in parentheses). It can be found that the RMSE is 9.5 kJ/mol, which is slightly larger than wB97/6-

311++G(2df,2p)//B3LYP/6-31+G(d) level (9.3 kJ/mol).

The excellent linear relationship between wB97 C-O BDEs in ethers and experimental ones is shown in Figure 1, in which the correlation coefficient square (R^2) is 0.982.

In summary, we successfully recommended the wB97/6-311++G (2df, 2p)//B3LYP/6-31+G(d) level to investigate the C(sp²)-O BDEs as well as the substituent effect in ethers/phenols.

Table 2. The correlations between theoretical with experimental C-O BDEs by 26 DFT methods

DFT methods	MD(kJ/mol)	MAD(kJ/mol)	RMSE(kJ/mol)
B3P86	-14.5	15.4	18.6
BMK	-4.4	9.4	11.3
M05	-14.5	15.4	18.6
M06-L	-23.5	23.6	26.1
M06-2X	26.2	29.8	41.2
BH&HLYP	-22.3	29.2	35.5
B3LYP	-35.3	35.3	45.4
CAM-B3LYP	-16.6	16.9	19.4
B3LYP-D3	-16.8	17.1	19.9
TPSS1KCIS	-12.4	25.7	28.5
B97-1	-18.3	18.7	21.2
B97-2	-21.7	21.8	25.1
B98	-22.8	22.8	25.2
B97-D	-29.8	29.8	31.3
B97-D3	-25.5	25.5	27.8
wB97	-2.4(-3.5)	8.2(7.3)	9.3(9.5)
wB97X	-7.4	9.7	11.7
wB97X-D	-0.02	13.4	15.3
PBE1PBE	-17.6	17.9	21.1
MPW1P86	-12.5	15.8	20.4
MPW1B95	-3.8	10.9	12.8
MPWCIS1K	-5.2	26.8	28.7
MPW1K	-26.9	26.9	29.5

MPWB1K	-3.5	10.9	12.9
MPWLYP1M	-17.5	25.0	29.3
MPW1KCIS	-24.7	24.7	28.1

Note: The values in parentheses are calculated at wB97/6-311++G(2df,2p)/wB97/6-31+G(d) level.

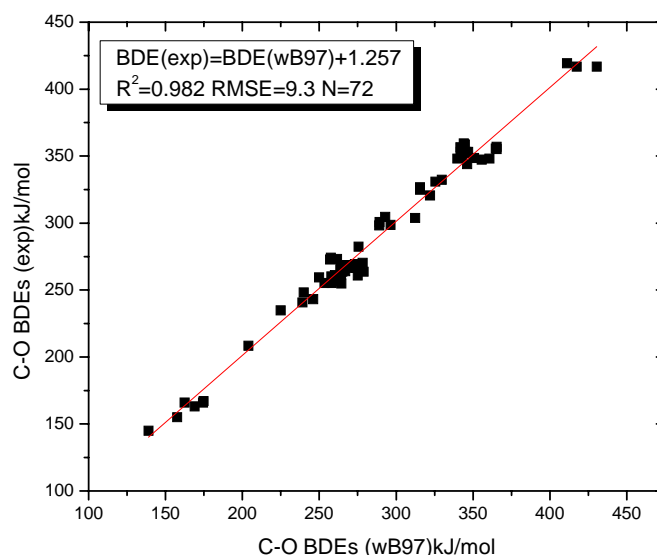


Figure. 1 Correlation between the wB97 and experimental C-O BDEs.

3.3 C(sp²)-O BDE prediction and substituent effect of alkenyl ethers

The C-O cleavage of alkenyl ethers with different substituents (R₁, R₂, R₃ and R₄) is depicted in Figure 2, in which the four substituents can all influence C-O BDEs. It can be seen that the R₃ and R₄ groups, which are at the site of C-O bond, play a direct role in C-O BDEs. By comparison, the R₁ and R₂ have the remote effect on the C-O activation. The alkenyl C(sp²)-O BDEs of different substituents with different properties⁵⁰ in ethers can help us to better understand synthetic organic reactions.

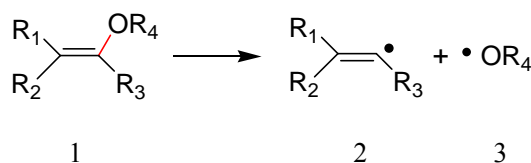


Figure.2 The C(sp²)-O cleavage of alkenyl ethers with different substituents(R₁, R₂, R₃ and R₄).

Firstly, the remote impact of different substituent R₁ and R₂ on C-O BDEs with the same R₃ and R₄ (–CH₃) are discussed, and the results at the wB97/6-311++G(2df, 2p)/B3LYP/6-31+G(d) level are shown in Table 3. It can be found that the range of C-O BDEs in Table 3 are from 377.1 kJ/mol to 426.5 kJ/mol, and there is a 49.4 kJ/mol gap.

As we all know, the alkenyl ethers 1 (in Figure 2) possibly have two conformations, (*Z*)- type and (*E*)- type. In the Table 3, the BDEs of the (*E*)- type conformations with different R_1 and R_2 are denoted in bold, and the ones of the (*Z*)- type are denoted in brackets. We can find that the C-O BDEs of (*Z*)- type are smaller than the (*E*)- ones, and the BDE differences between the two types are in the range of 1.1 kJ/mol to 13.1 kJ/mol. For example, when the $R_1 = \text{CH}_3$ and $R_2 = \text{CF}_3$, the C-O BDE is 388.3 kJ/mol, which is slightly larger than (*Z*)- type of 380.0 kJ/mol ($R_1 = \text{CF}_3$ and $R_2 = \text{CH}_3$). The two larger substituents of the (*E*)- type conformations are in the different side, which may cause the smaller steric hindrance. So the higher stability of the (*E*)- type conformations leads to larger C-O BDEs.

Comparing the C-O BDEs of the same type with different R_1 and R_2 , it can be seen that the $-\text{CN}$ group would greatly increase the C-O BDEs. Especially, the largest BDE 426.5 kJ/mol is found in the case of $R_1 = \text{CN}$ and $R_2 = \text{CN}$. It reveals that the strong electron-withdrawing effect as well as conjugate effect of $-\text{CN}$ group both act on the C-O BDE. For other groups, including typical electron-donating groups, such as $-\text{CH}_3$, $-\text{F}$, conjugate effect group $-\text{Ph}$, and $-\text{CF}_3$, the C-O BDE discrepancies are less than 8 kJ/mol.

Table 3. The C-O BDEs of substituted ethers with different R_1 and R_2

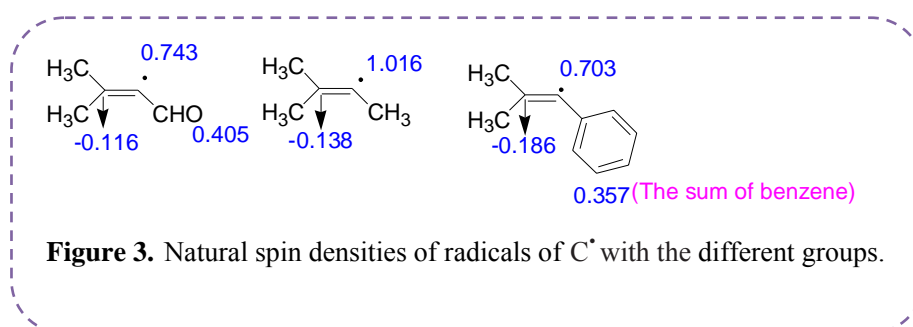
Structure	C-O BDEs (kJ/mol)					
	<div><div>R₁</div><div>R₂</div></div>	−CH ₃	−F	−CF ₃	−CN	−Ph
<div><div><div>R₁</div><div>R₂</div></div><div><div>OCH₃</div><div>CH₃</div></div></div>	−CH ₃	386.4	(386.0)	(380.0)	(392.6)	(381.7)
	−F	390.8	387.2	383.3	402.8	384.8
	−CF ₃	388.3	(381.7)	389.5	410.5	385.5
	−CN	405.7	(397.8)	(406.7)	426.5	398.7
	−Ph	385.8	(384.5)	(377.1)	(391.5)	384.4

* (*E*)- type in bold, (*Z*)- type in brackets.

Secondly, in order to investigate the effect of R_3 and R_4 on C-O BDEs, we fixed the R_1 and R_2 as both $-\text{CH}_3$ group for convenience. The results of C-O BDEs in alkenyl ethers with different R_3 and R_4 at wB97/6-311++G (2df, 2p)//B3LYP/6-31+G(d) level are summarized in the Table 4. After the natural bond orbital (NBO) analysis⁵¹ conducted at wB97/6-31+G(d) level, the values of $q_C \times q_O$ are also shown in the table, where the q_C and q_O denote the natural charges of C and O atoms of C-O bond in ethers respectively.

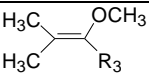
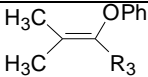
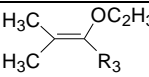
In the Table 4, the C-O BDEs of ethers with different R_3 and R_4 are in the range of 270.2~428.1 kJ/mol, and there is a large difference of 157.9 kJ/mol. The maximum is discovered in No.6 ($R_4=\text{CH}_3$, $R_3=\text{F}$) and the minimum occurs in No.30 ($R_4=\text{C}_2\text{H}_5$, $R_3=\text{Ph}$), which indicated that the R_3 and R_4 play a vital role in C-O BDEs.

When the $R_4=\text{CH}_3$ (No.1~10), it can be found that the electron-withdrawing groups (EWGs) of R_3 including $-\text{CF}_3$, $-\text{CN}$, $-\text{CHO}$, and $-\text{COOH}$ (No.1~4) can decrease the C-O BDEs of ethers. By contrast, the electron-donating groups (EDGs) of R_3 including $-\text{CH}_3$, $-\text{NH}_2$, $-\text{OH}$, $-\text{F}$, and $-\text{OCH}_3$ (No. 5-9) can obviously increase the BDEs. For example, for the $R_3=\text{OH}$, the C-O BDE is 406.3 kJ/mol, while for the $R_3=\text{CN}$, the C-O BDE is 375.4 kJ/mol, and there is 30.9 kJ/mol gap. It may because the EWGs can directly disperse the electron density of the radical center, which leads to the stability enhancement of radical 2 (Figure 2). It should be mentioned that there is the largest C-O BDEs when the $R_3=\text{F}$ (428.1 kJ/mol), implying that the $-\text{F}$ exhibits the strong electron-donating effect, which may due to the small atomic radius. For the conjugation effect group (CEG) ($R_3=\text{Ph}$, No.10), there is a smaller C-O BDE prediction of 348.0 kJ/mol, which shows that the π - π conjugated effect between the phenyl group and the $\text{C}=\text{C}$ bond, as well as the steric hindrance of $-\text{Ph}$ both have influences on C-O BDEs. The same phenomena can be found in the $R_4=\text{Ph}$ (No.11~20) and $R_4=\text{C}_2\text{H}_5$ (No.21~30). The natural spin densities of the radical center C^\bullet of radical 2 with three R_3 groups ($-\text{CH}_3$, $-\text{CHO}$, $-\text{Ph}$) are listed in Figure 3. The different changing patterns of R_3 on C-O BDEs can be explained as follows: When the $R_3=\text{CH}_3$ (EDG), the natural spin densities mainly concentrated on the C^\bullet radical center (1.016). While, for the $R_3=\text{CHO}$ (EWG) and $R_3=\text{Ph}$ (CEG), the natural spin densities of the radical center C^\bullet are 0.743 and 0.703 respectively, which are obviously delocalized onto the $-\text{CHO}$ and $-\text{Ph}$ groups. The stronger delocalization effect of the radical center can lead to the smaller C-O BDEs of these ethers.



Interestingly, different R_4 have large influences on the C-O BDEs of ethers. When the R_4 are $-\text{Ph}$ and $-\text{C}_2\text{H}_5$, the overall values are much smaller than $-\text{CH}_3$. For example, when the $R_3 = \text{CH}_3$ and $R_4 = \text{C}_2\text{H}_5$, the C-O BDE is 296.1 kJ/mol, which is much smaller than the 385.5 kJ/mol ($R_3 = \text{CH}_3$ and $R_4 = \text{CH}_3$). There is about 90 kJ/mol C-O BDE discrepancy! In order to get a further explanation about the effect of R_4 , the natural spin densities of O atoms in radicals 3 with different R_4 are listed in Figure 4. For $R_4 = \text{CH}_3$, the natural spin densities mainly concentrated on the O radical center (0.930). However, for the $-\text{Ph}$ and $-\text{C}_2\text{H}_5$ groups, the natural spin densities of the radical center O are 0.425 and 0.351 respectively, which are strongly delocalized onto the C=C bonds. It can be concluded that the conjugate effect of R_4 group can obviously decrease the C-O BDEs.

Table 4. The C-O BDEs of substituted ethers with different R_3 and R_4 as well as the values of $q_C \times q_O / e^2$

R_3	No.			No.			No.		
		BDE (kJ/mol)	$q_C \times q_O$		BDE (kJ/mol)	$q_C \times q_O$		BDE (kJ/mol)	$q_C \times q_O$
$-\text{CF}_3$	1	385.3	-0.095	11	309.6	-0.091	21	296.1	-0.100
$-\text{CN}$	2	375.4	-0.091	12	291.8	-0.080	22	279.0	-0.083
$-\text{CHO}$	3	375.8	-0.093	13	296.5	-0.082	23	284.9	-0.084
$-\text{COOH}$	4	383.3	-0.087	14	305.2	-0.078	24	291.2	-0.072
$-\text{CH}_3$	5	386.4	-0.175	15	315.2	-0.158	55	300.2	-0.161
$-\text{F}$	6	428.1	-0.410	16	344.8	-0.366	66	331.8	-0.374
$-\text{NH}_2$	7	386.0	-0.222	17	311.5	-0.218	27	297.7	-0.228
$-\text{OCH}_3$	8	402.1	-0.346	18	324.5	-0.325	28	311.8	-0.330
$-\text{OH}$	9	406.3	-0.346	10	329.3	-0.322	29	315.5	-0.327
$-\text{Ph}$	10	348.0	-0.172	20	279.2	-0.153	30	270.2	-0.153

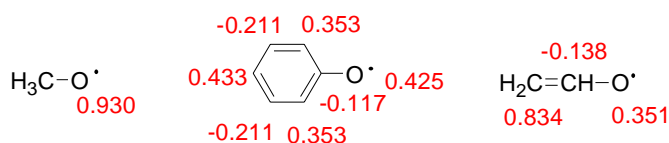


Figure 4. Natural spin densities of radicals of O[•] with the different groups.

Furthermore, the $q_C \times q_O$ values range from -0.410 to -0.072 in Table 4. The NBO analysis produced three good linear correlations between the C-O BDEs and $q_C \times q_O$ values for each R_4 group, excluding the three points marked in the figure (No.10, No.20 and No.30). The relationships are depicted in Figure 5 and the correlation coefficients(R) are 0.913, 0.903 and 0.909 respectively. Generally, the larger C-O BDEs would result in larger absolute $q_C \times q_O$, which reveals the essence of C-O bond in alkenyl ethers.

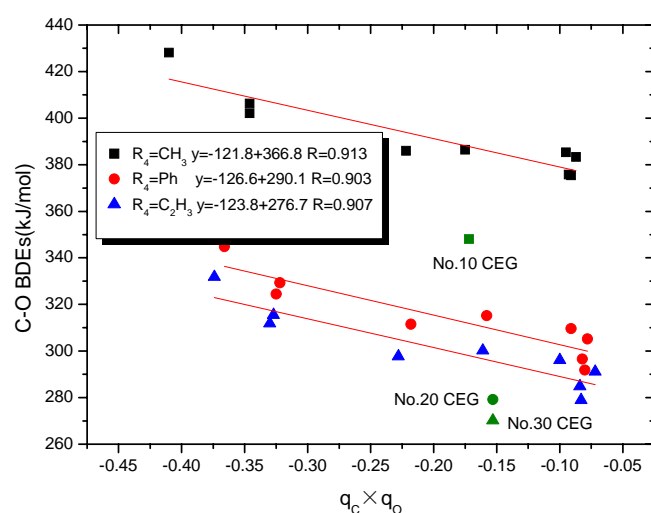
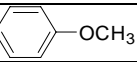
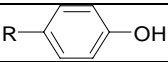


Figure 5. Correlations between the C-O BDEs and $q_C \times q_O$ values for each R_4 group.

3.4 C(sp²)-O BDE prediction and *para*- substituent effect of phenyl ethers/phenols

Since the substituted aryl ethers/phenols with various groups are commonly used as substrates involved in the cross-coupling reactions, the C(sp²)-O BDE prediction and substituent effect(especially the *para*-position effect) can provide us effective understanding of C-O cleavage. Therefore, the *para*-substituted phenyl ethers/phenols are chosen as the calculating set, and the corresponding C(sp²)-O BDEs at wB97/6-311++G (2df, 2p)//B3LYP/6-31+G(d) level are listed in the Table 5.

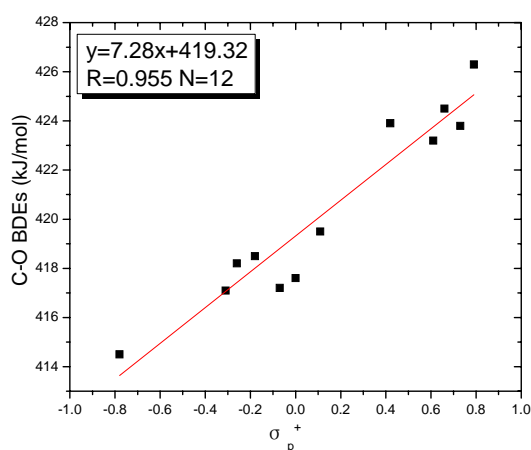
Table 5. The C(sp²)-O BDEs as well as the GE, RE values of substituted phenyl ethers/phenols(kJ/mol)

R	σ_p^+	R- 			R- 		
		BDEs(kJ/mol)	GE	RE	BDEs(kJ/mol)	GE	RE
-NO ₂	0.79	426.3	5.9	-2.8	475.4	4.1	-2.8

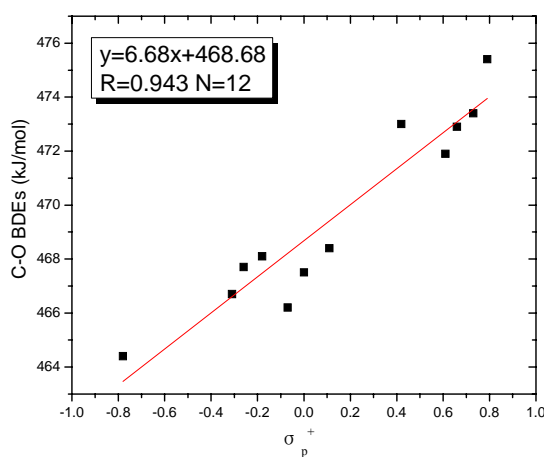
-CHO	0.73	423.8	5.8	-0.4	473.4	5.5	-0.4
-CN	0.66	424.5	5.0	-2.0	472.9	3.5	-2.0
-CF ₃	0.61	423.2	3.8	-1.8	471.9	2.6	-1.8
-COOH	0.42	423.9	5.9	-0.4	473.0	5.1	-0.4
-Cl	0.11	419.5	-1.6	-3.6	468.4	-2.7	-3.6
-H	0	417.6	0	0	467.5	0	0
-F	-0.07	417.2	-5.3	-4.9	466.2	-6.2	-4.9
-Ph	-0.18	418.5	-0.5	-1.4	468.1	-0.8	-1.4
-C(CH ₃) ₃	-0.26	418.2	-1.0	-1.6	467.7	-1.4	-1.6
-CH ₃	-0.31	417.1	-1.9	-1.4	466.7	-2.3	-1.4
-OCH ₃	-0.78	414.5	-7.0	-5.0	464.4	-8.0	-5.0

Hammett analysis⁵² would not only provide us a way to predict the BDE changing patterns, but also can explain the different influencing factors. The Brown-Okamoto substituent constant σ_p^+ values mainly based on the solvolysis of substituted *t*-cumyl chlorides⁵³ are listed in the Table 5. In the present study, two excellent linear relationships between C(sp²)-O BDEs of *p*-R-C₆H₄-OCH₃ and *p*-R-C₆H₄-OH with substituent constant (σ_p^+) were found, in which the correlation coefficients (R) are 0.955 and 0.943 respectively. The correlations are depicted in Figure 6.

The slope, expressed by ρ^+ reveals the BDE sensitivity of electronic effect of remote substituents (R). It is found that the ρ^+ values of phenyl ethers and phenols are 7.28 and 6.68 separately, which reveals that the C-O BDE of phenyl ethers has larger sensitivity to different *para*-substituents.



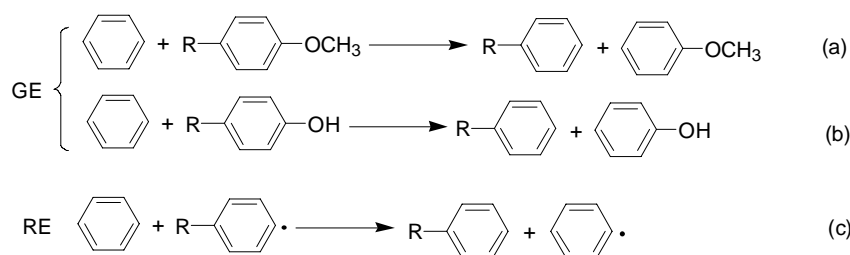
(a)



(b)

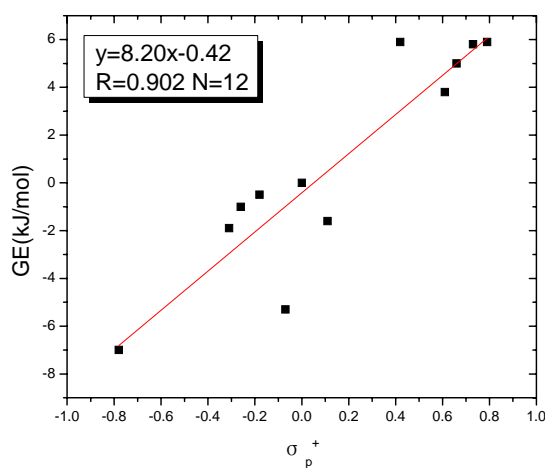
Figure 6. Correlations between C-O BDEs and σ_p^+ of ethers(a)/phenols(b).

As shown in Table 5, by comparing with the EDGs like $-\text{CH}_3$ and $-\text{OCH}_3$, the EWGs of R such as $-\text{CF}_3$ and $-\text{CHO}$ can slightly increase the C-O BDEs for phenyl ethers and phenols. It may be because the EWGs can lead to the stability enhancement of molecules than the radicals. In general, to further understand the essence of the substituent effect, it is reasonable to separate the remote substituent effect into the ground effect (GE) and the radical effect (RE). The GE and RE definitions for phenyl ethers/phenols are determined by the enthalpy changes in Scheme 2. It is worth mentioning that a positive GE (RE) value shows that the R can facilitate the molecules (radicals) stability while a negative value indicates the stability decrease. The calculated GE, RE values of phenyl ethers and phenols for different R groups are also listed in the Table 5. From this table, for both phenyl ethers and phenols, the GE values of EWGs are generally positive and the ones of EDGs are negative, which indicated that the EWGs can stabilize the molecules while the EDGs are disadvantageous for the molecule stability. It can be explained as follows: On the one hand, when the R is EDG, the two groups of R and the $-\text{OCH}_3$ or $-\text{OH}$ (in the *para*-position of R) with the same property will appear push-push effect, which can destabilize the molecules. On the other hand, if the R is EWG, the push-pull effect will display larger C-O BDEs.⁵⁴

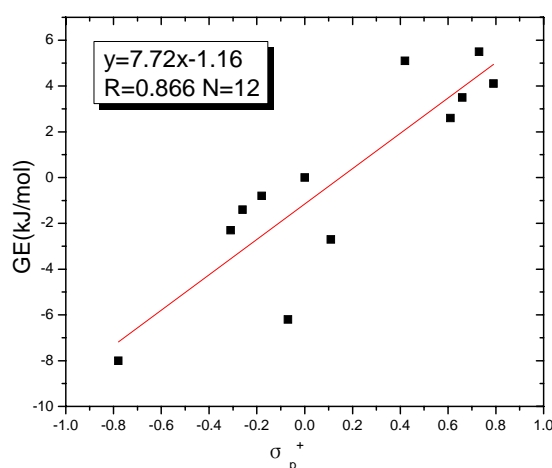


Scheme 2. The GE of phenyl ethers(a) , phenol(b) and the RE (c) of these compounds.

We correlated both GE and RE values of phenyl ethers and phenols in Table 5 with the substituent constant σ_p^+ . It can be seen that there are two linear relationships between GE and σ_p^+ of the two types (Figure 7), and the correlation coefficients (R) are 0.902 for ethers and 0.866 for phenols. The two linear relationships are much better than the correlation between RE and σ_p^+ ($RE=1.28\sigma_p^+-2.29$, $R=0.248$). Comparing the ρ^+ (GE) values of phenyl ethers (8.20) and phenols (7.72) with the ρ^+ (RE) (1.28), we can draw the conclusion that the GE plays a strong role in the C-O BDEs of phenyl ethers/phenols rather than RE. In addition, the phenyl ethers have a stronger GE effect on C-O BDEs than phenols.



(a)



(b)

Figure 7. Correlations between GE and σ_p^+ of phenyl ethers(a) and phenols(b).

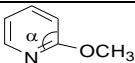
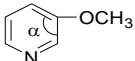
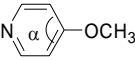
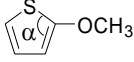
3.5 C(sp²)-O BDE prediction of heterocyclic ethers

The heterocyclic compounds have arousing great interests because of the wide range of applications in the field of pharmaceuticals, pesticides and materials.⁵⁵ Therefore we predicted the C(sp²)-O BDEs of several typical heterocyclic ethers using the wB97/6-311++G (2df, 2p)//B3LYP/6-31+G(d) and the results are summarized in Table 6.

From the table 6, the C-O BDEs of heterocyclic ethers are in the range of 410.9~444.7 kJ/mol. On the one hand, the pyridine, pyrrole, furan and thiofuran rings exhibit different C-O BDEs. For pyridine ethers, when the C-O bond is located at the *ortho*-position of N atom, the BDE is larger than the *para*- and *meta*- positions. In pyrrole, furan, and thiofuran ethers, the same phenomenon is also found. On the other hand, for the five-membered heterocyclic ethers, the C-O BDEs of pyrrole are close to furan, which are much larger than thiofuran(about 20 kJ/mol). The discrepancy can be caused by the electronegativity differences of N, O, S atoms.

In addition, the bond angles α at the cleavage site of molecules and radicals as well as bond angle change $\Delta\alpha$ (mol-rad) are also shown in Table 6. The trends in bond angle changes with the C-O BDEs for 6 five-membered heterocyclic ethers are depicted in Figure 8, which shows that the larger bond angle change $\Delta\alpha$ will lead to a smaller C-O BDE in five-membered heterocyclic ethers. While for six-membered heterocyclic ethers, the trends are not obvious. For example, the C-O BDE of furan ether (No.6) is 444.7 kJ/mol, and the bond angle change $\Delta\alpha$ is 2.8, which is smaller than the 5.0 value in thiofuran ether (No.5) with the BDE of 417.2 kJ/mol. The similar trends for C-H BDEs in aromatic hydrocarbons⁵⁶ as well as the carbon-halogen BDEs in halo-heterocycles⁴⁹ are found.

Table 6. The C(sp²)-O BDE predictions and bond angles for typical heterocyclic ethers

No.	heterocyclic ethers	α (mol)	α (rad)	$\Delta\alpha$ (mol-rad)	BDE(kJ/mol)
1		123.8	126.6	2.8	424.9
2		118.3	123.8	5.5	418.8
3		118.8	123.9	5.1	410.9
4		112.3	115.7	3.4	424.3

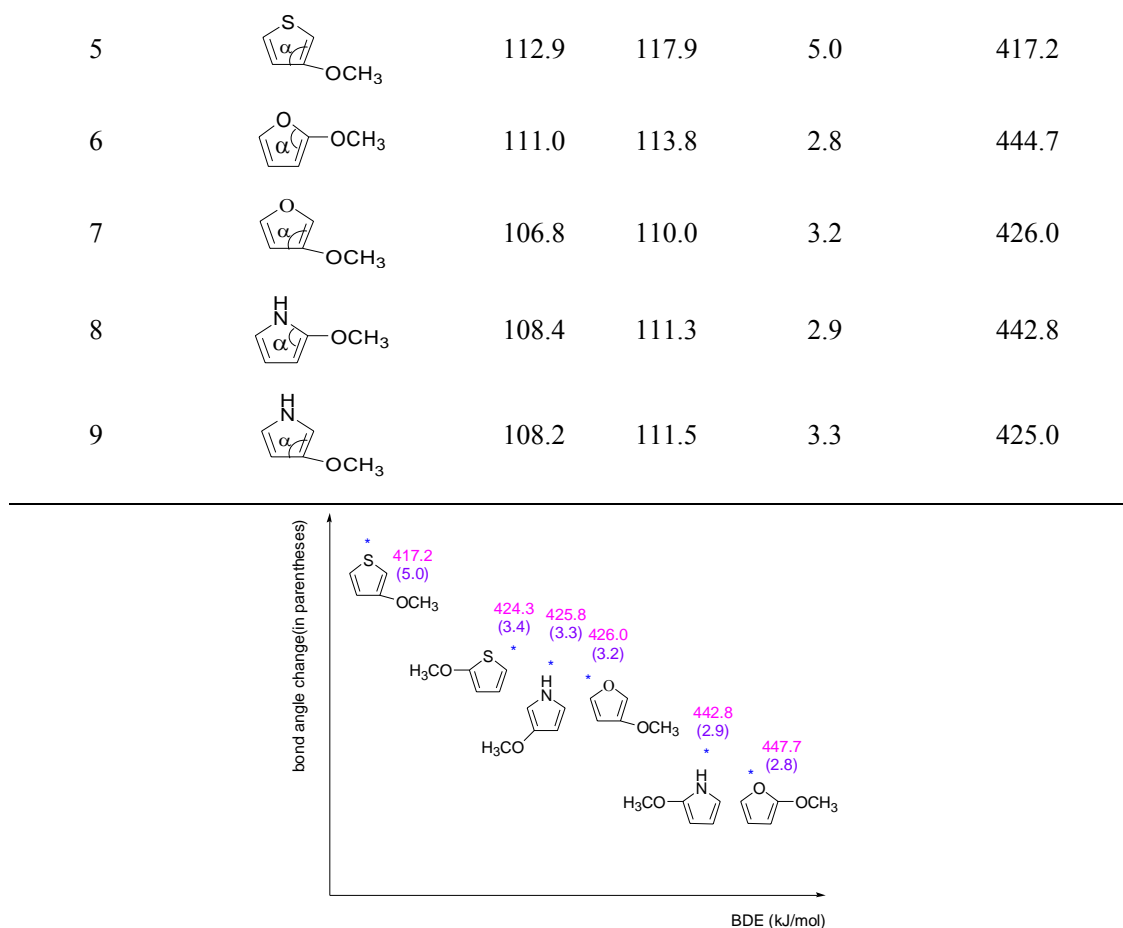


Figure 8. The trends in bond angle changes with BDEs for five-membered heterocyclic ethers .

4 Conclusion

The $C(sp^2)$ -O homolytic BDEs of ethers and phenols are significant to the understanding of C-O activation in cross-coupling reactions. In the present study, the composite high-level *ab initio* methods including G4, G3, CBS-Q and CBS-4M were used to evaluate the 19 C-O bond dissociation enthalpies(BDEs) of ethers, the G4 method gave the smallest root mean square error (RMSE) of 6.9 kJ/mol. Then, 72 C-O BDEs were calculated by 26 density function theory (DFT) methods, which indicated that wB97 method can provide the highest precision (RMSE= 9.3 kJ/mol). Afterwards, the $C(sp^2)$ -O BDE predictions and the substituent effects of alkenyl ethers, *para*-position phenyl ethers/phenols as well as several typical heterocyclic ethers were investigated in detail by using wB97 method. In addition, the natural bond orbital (NBO) analysis further disclosed the essence of the substituent effects on C-O BDEs. The major results are summarized as follow.

(1)For alkenyl ethers, the different R_1 , R_2 , R_3 and R_4 play significant effects on C-O BDEs. Firstly, comparing the C-O BDEs of different R_1 and R_2 , the -CN group would greatly increase the C-O BDEs. Secondly, the electron-withdrawing groups (EWGs)

of R_3 can decrease the $C(sp^2)$ -O BDEs. By contrast, the electron-donating groups (EDGs) of R_3 can obviously increase the BDEs. It is because the EWGs can directly disperse the electron density of the radical center, which leads to the stability enhancement of radical. Lastly, the conjugate effect of R_4 group can obviously decrease the C-O BDEs. In addition, the NBO analysis produced three good linear correlations between the C-O BDEs and $q_C \times q_O$ values for each R_4 group with different R_3 .

(2) For the *para*-position phenyl ethers and phenols, excellent linear relationships between the C-O BDEs with substituent constant σ_p^+ were found. By comparing with the EDGs, the EWGs of remote substituent R can slightly increase the C-O BDEs.

(3) For several five-membered heterocyclic typical heterocyclic ethers, when the $C(sp^2)$ -O bond is located at the *ortho*- position of N, O, S atom, the BDE is the largest. In addition, the larger bond angle change will lead to a smaller C-O BDE for heterocyclic ethers.

Acknowledgement

This project is sponsored by Shanghai University of Engineering Science Innovation Fund for Graduate Students (No.14KY0403). We also thank Shanghai Supercomputer Center for the computational resources.

Supporting Information

The 72 C-O BDEs calculated by 26 DFT methods.

References

- (a) B.-T. Guan, S.-K. Xiang, B.-Q. Wang, Z.-P. Sun, Y. Wang, K.-Q. Zhao and Z.-J. Shi, *J. Am. Chem. Soc.*, 2008, **130**, 3268–3269. (b) M. Tobisu, T. Shimasaki and N. Chatani, *Angew. Chem. Int. Ed.*, 2008, **47**, 4866–4869. (c) Z. Li, S.-L. Zhang, Y. Fu, Q.-X. Guo and L. Liu, *J. Am. Chem. Soc.*, 2009, **131**, 8815–8823. (d) H. Kinuta, M. Tobisu and N. Chatani, *J. Am. Chem. Soc.*, 2015, **137**, 1593–1600. (e) M. Trivedi, S. K. Ujjain, R. K. Sharma, G. Singh, A. Kumar and N. P. Rath, *New J. Chem.*, 2014, **38**, 4267–4274.
- (a) B. M. Rosen, K. W. Quasdorf, D. A. Wilson, N. Zhang, A.-M. Resmerita, N. K. Garg and V. Percec, *Chem. Rev.*, 2011, **111**, 1346–1416. (b) B.-J. Li, D.-G. Yu, C.-L. Sun and Z.-J. Shi, *Chem. Eur. J.*, 2011, **17**, 1728–1759. (c) Y.-J. Liu, S. K. Park, Y. Xiao and J. Chae, *Org. Biomol. Chem.*,

- 2014, **12**, 4747–4753. (d) Z. Li, and L. Liu, *Chin. J. Catal.*, 2015, **36**, 3–14.
- 3 (a) E. Wenkert, E. L. Michelotti and C. S. Swindell, *J. Am. Chem. Soc.*, 1979, **101**, 2246–2247. (b) E. Wenkert, E. L. Michelotti, C. S. Swindell and M. Tingoli, *J. Org. Chem.*, 1984, **49**, 4894–4899.
- 4 E. Wenkert, V. F. Ferreira, E. L. Michelotti and M. Tingoli, *J. Org. Chem.*, 1985, **50**, 719–721.
- 5 R. A. W. Johnstone and W. N. McLean, *Tetrahedron Lett.*, 1988, **29**, 5553–5556.
- 6 B.-T. Guan, S.-K. Xiang, T. Wu, Z.-P. Sun, B.-Q. Wang, K.-Q. Zhao and Z.-J. Shi, *Chem. Commun.*, 2008, **12**, 1437–1439.
- 7 M. Tobisu, T. Shimasaki and N. Chatani, *Angew. Chem. Int. Ed.* 2008, **47**, 4866–4969.
- 8 M. Tobisu, T. Shimasaki and N. Chatani, *Chem. Lett.*, 2009, **38**, 710–711.
- 9 D.-G. Yu, B.-J. Li, S.-F. Zheng, B.-T. Guan, B.-Q. Wang and Z.-J. Shi, *Angew. Chem., Int. Ed.*, 2010, **49**, 4566–4570.
- 10 (a) K. B. Wiberg and G. A. Petersson, *J. Phys. Chem. A*, 2014, **118**, 2353–2359. (b) M. Morris, B. Chan and L. Radom, *J. Phys. Chem. A*, 2014, **118**, 2810–2819. (c) H.-F. Ji and H.-Y. Zhang, *New. J. Chem.*, 2005, **29**, 535–537. (d) H.-Y. Zhang, *New. J. Chem.*, 2004, **28**, 1284–1285. (e) C. J. Hayes and C. M. Hadad, *J. Phys. Chem. A*, 2009, **113**, 12370–12379. (f) B. Chan, and L. Radom, *J. Phys. Chem. A*, 2012, **116**, 4975–4986. (g) B. Chan, and L. Radom, *J. Phys. Chem. A*, 2013, **117**, 3666–3675.
- 11 D. A. Pratt, M. I. Heer, P. Mulder and K. U. Ingold, *J. Am. Chem. Soc.*, 2001, **123**, 5518–5526.
- 12 S. J. Blanksby and G. B. Ellison, *Acc. Chem. Res.*, 2003, **36**, 255–263.
- 13 (a) Y.-H. Cheng, X. Zhao, K.-S. Song, L. Liu and Q.-X. Guo, *J. Org. Chem.*, 2002, **67**, 6638–6645. (b) K.-S. Song, L. Liu and Q.-X. Guo, *J. Org. Chem.*, 2003, **68**, 262–266.
- 14 L. A. Curtiss, P. C. Redfern and K. Raghavachari, *J. Chem. Phys.*, 2007, **126**, 084108-1–084108-12.
- 15 L. A. Curtiss, K. Raghavachari, P. C. Redfern, V. Rassolov and J. A. Pople, *J. Chem. Phys.*, 1998, **109**, 7764–7776.
- 16 Y. Fu, Y. Mou, B.-L. Lin, L. Liu and Q.-X. Guo, *J. Phys. Chem. A*, 2002, **106**, 12386–12392.
- 17 (a) J. W. Ochterski, G. A. Petersson and K. B. Wiberg, *J. Am. Chem. Soc.*, 1995, **117**, 11299–11308. (b) A. D. Becke, *J. Chem. Phys.*, 1993, **98**, 5648–5652.
- 18 (a) A. Modelli, L. Mussoni, and D. Fabbri, *J. Phys. Chem. A*, 2006, **110**, 6482–6486. (b) Y. Fu, L. Liu, H.-Z. Yu, Wang, Y.-M and Q.-X. Guo, *J. Am. Chem. Soc.*, 2005, **127**, 7227–7234. (c) Y. Jiang, H. Yu, Y. Fu and L. Liu, *Sci. China Chem.*, 2015, **58**, 673–683.
- 19 J. P. Perdew, *Phys. Rev. B*, 1986, **33**, 8822–8824.
- 20 A. D. Boese and J. M. L. Martin, *J. Chem. Phys. B*, 2004, **8**, 3405–3416.
- 21 Y. Zhao, N. E. Schultz and D. G. Truhlar, *J. Chem. Phys.*, 2005, **123**, 161103-1–161103-4.
- 22 A. D. Becke, *Phys. Rev. A*, 1988, **38**, 3098–3100.
- 23 C. T. Lee, W. T. Yang and R. G. Parr, *Phys. Rev. B*, 1988, **37**, 785–789.
- 24 Y. Zhao and D. G. Truhlar, *J. Chem. Phys.*, 2006, **125**, 194101-1–194101-18.
- 25 Y. Zhao, B. J. Lynch and D. G. Truhlar, *Phys. Chem. Chem. Phys.*, 2005, **7**, 43–52.

- 26 A. D. Becke, *J. Chem. Phys.*, 1997, **107**, 8554–8560.
- 27 P. J. Wilson, T. J. Bradley, and D. J. Tozer, *J. Chem. Phys.*, 2001, **115**, 9233–9242.
- 28 H. L. Schmider and A. D. Becke, *J. Chem. Phys.*, 1998, **108**, 9624–9631.
- 29 J.-D. Chai and M. Head-Gordon, *J. Chem. Phys.*, 2008, **128**, 084106-1–084106-15.
- 30 J.-D. Chai and M. Head-Gordon, *Phys. Chem. Chem. Phys.*, 2008, **10**, 6615–6623.
- 31 M. Ernzerhof and G. E. Scuseria, *J. Chem. Phys.*, 1999, **110**, 5029–5036.
- 32 J. P. Perdew, K. Burke and Y. Wang, *Phys. Rev. B*, 1996, **54**, 16533–16539.
- 33 Y. Zhao and D. G. Truhlar, *J. Phys. Chem. A*, 2004, **108**, 6908–6918.
- 34 Y. Zhao, N. González-García and D. G. Truhlar, *J. Phys. Chem. A*, 2005, **109**, 2012–2018.
- 35 S. Grimme, *J. Comput. Chem.*, 2006, **27**, 1787–1799.
- 36 B. J. Lynch, P. L. Fast, M. Harris and D. G. Truhlar, *J. Phys. Chem. A*, 2000, **104**, 4811–4815.
- 37 C. Schultz-Fademrecht, M. A. Tius, S. Grimme, B. Wibbeling and D. Hoppe, *Angew. Chem. Int. Ed.*, 2002, **41**, 1532–1535.
- 38 T. Yanai, D. P. Tew, and N. C. Handy, *Chem. Phys. Lett.*, 2004, **393**, 51–57.
- 39 S. Grimme, J. Antony, S. Ehrlich, and H. Krieg, *J. Chem. Phys.*, 2010, **132**, 154104-1–154104-19.
- 40 A. Austin, G. A. Petersson, M. J. Frisch, F. J. Dobek, G. Scalmani, and K. Throssell, *J. Chem. Theory Comput.*, 2012, **8**, 4989–5007.
- 41 Y. Zhao, and D. G. Truhlar, *Theor. Chem. Acc.*, 2008, **120**, 215–241.
- 42 M. J. Frisch, G. W. Trucks, H. B. Schlegel, G. E. Scuseria, M. A. Robb, J. R. Cheeseman, G. Scalmani, V. Barone, B. Mennucci, G. A. Petersson, H. Nakatsuji, M. Caricato, X. Li, H. P. Hratchian, A. F. Izmaylov, J. Bloino, G. Zheng, J. L. Sonnenberg, M. Hada, M. Ehara, K. Toyota, R. Fukuda, J. Hasegawa, M. Ishida, T. Nakajima, Y. Honda, O. Kitao, H. Nakai, T. Vreven, J. A. Montgomery, Jr., J. E. Peralta, F. Ogliaro, M. Bearpark, J. J. Heyd, E. Brothers, K. N. Kudin, V. N. Staroverov, T. Keith, R. Kobayashi, J. Normand, K. Rahavachari, A. Rendell, J. C. Burant, S. S. Iyengar, J. Tomasi, M. Cossi, N. Rega, J. M. Millam, M. Klene, J. E. Knox, J. B. Cross, V. Bakken, C. Adamo, J. Jaramillo, R. Gomperts, R. E. Stratmann, O. Yazyev, A. J. Austin, R. Cammi, C. Pomelli, J. W. Ochterski, R. L. Martin, K. Morokuma, V. G. Zakrzewski, G. A. Voth, P. Salvador, J. J. Dannenberg, S. Dapprich, A. D. Daniels, Ö. Farkas, J. B. Foresman, J. V. Ortiz, J. Cioslowski and D. J. Fox, Gaussian 09, Revision D.01, Gaussian, Inc. Wallingford CT, 2009.
- 43 (a) J. A. Pople, M. Head-Gordon, D. J. Fox, K. Raghavachari and L. A. Curtiss, *J. Chem. Phys.*, 1989, **90**, 5622–5629. (b) L. A. Curtiss, K. Raghavachari, G. W. Trucks and J. A. Pople, *J. Chem. Phys.*, 1991, **94**, 7221–7230. (c) L. A. Curtiss, K. Raghavachari, P. C. Redfern, V. Rassolov and J. A. Pople, *J. Chem. Phys.*, 1998, **109**, 7764–7776. (d) B. Chan, J. Deng and L. Radom, *J. Chem. Theory Comput.*, 2011, **7**, 112–120.
- 44 (a) J. W. Ochterski, G. A. Petersson and J. A. Jr. Montgomery, *J. Chem. Phys.*, 1996, **104**, 2598–2619. (b) J. A. Jr. Montgomery, M. J. Frisch, J. W. Ochterski and G. A. Petersson, *J. Chem. Phys.*, 1999, **110**, 2822–2827. (c) G. P. Wood, L. Radom, G. A. Petersson, E. C. Barnes, M. J. Frisch and J. A. Jr. Montgomery, *J. Chem. Phys.*, 2006, **125**, 094106-1–094106-16.

- 45 (a) J. W. Ochterski, G. A. Petersson and K. B. Wiberg, *J. Am. Chem. Soc.*, 1995, **117**, 11299–11308. (b) L. A. Curtiss, P. C. Redfern and K. Raghavachari, *J. Chem. Phys.*, 2005, **123**, 124107-1–124107-12. (c) A. G. Baboul, L. A. Curtiss, P. C. Redfern and K. Raghavachari, *J. Chem. Phys.*, 1999, **110**, 7650–7657. (d) D. Bond, *J. Org. Chem.*, 2007, **72**, 5555–5566. (f) W. Danikiewicz, *Int. J. Mass. Spectrom.*, 2009, **285**, 86–94.
- 46 Y.-R. Luo, *Comprehensive Handbook of Chemical Bond Energies*; CRC Press: Boca Raton, FL, 2007.
- 47 Y.-X. Wang and W.-R. Zheng, *J. Sulfur. Chem.*, 2015, **36**, 155–159.
- 48 (a) D. A. Pratt, J. H. Mills and N. A. Porter, *J. Am. Chem. Soc.*, 2003, **125**, 5801–5810. (b) F. Turecek, *J. Am. Chem. Soc.*, 2003, **125**, 5954–5963. (c) M. S. Alnajar, X.-M. Zhang, G. J. Gleicher, S. V. Truksa and J. A. Franz, *J. Org. Chem.*, 2002, **67**, 9016–9022.
- 49 Y. Garcia, F. Schoenebeck, C. Y. Legault, C. A. Merlic and K. N. Houk, *J. Am. Chem. Soc.*, 2009, **131**, 6632–6639.
- 50 (a) N. Chéron, R. Ramozzi, L. E. Kaïm, L. Grimaud and P. Fleurat-Lessard, *J. Phys. Chem. A*, 2013, **117**, 8035–8042. (b) W. Mbiya, I. Chipinda, P. D. Siegel, M. Mhike and R. H. Simoyi, *Chem. Res. Toxicol.*, 2013, **26**, 112–123.
- (c) A. S. Menon, D. J. Henry, T. Bally and L. Radom., *Org. Biomol. Chem.*, 2011, **9**, 3636–3657.
- 51 A. E. Reed, L. A. Curtiss and F. Weinhold, *Chem. Rev.*, 1988, **88**, 899–926.
- 52 (a) A. A. Zavitsas, D. W. Rogers and N. Matsunaga, *J. Org. Chem.*, 2007, **72**, 7091–7101. (b) L. Liu, Y. Fu, R.-Q. Li and Q.-X. Guo, *J. Chem. Inf. Comput. Sci.*, 2004, **44**, 652–657.
- 53 (a) L. Turi and J. J. Dannenberg, *J. Phys. Chem.*, 1993, **97**, 12197–12204. (b) K. B. Wiberg and K. E. Laidig, *J. Am. Chem. Soc.*, 1987, **109**, 5935–5943. (c) D. M. Pawar, D. Cain-Davis and E. A. Noe, *J. Org. Chem.*, 2007, **72**, 2003–2007.
- 54 (a) Y. Fu, L. Liu, B.-L. Lin, Y. Mou, Y.-H. Cheng and Q.-X. Guo, *J. Org. Chem.*, 2003, **68**, 4657–4662. (b) D. A. Pratt, G. A. Dilabio, P. Mulder and K. U. Ingold, *Acc. Chem. Res.*, 2004, **37**, 334–340.
- 55 (a) M. G. Hobbs, T. D. Forster, J. Borau-Garcia, C. J. Knapp, H. M. Tuononen and R. Roesler, *New. J. Chem.*, 2010, **34**, 1295–1308. (b) Y.-Y. Huang, S. Suzuki, G.-K. Liu, E. Tokunaga, M. Shiro and N. Shibata, *New J. Chem.*, 2011, **35**, 2614–2621.
- 56 C. Barckholtz, T. A. Barckholtz and C. M. Hadad, *J. Am. Chem. Soc.*, 1999, **121**, 491–500.